Inorg. Chem. **2003**, *42*, 2428–2439

Synthesis and Characterization of Three Novel Cation-Containing (NH_4^+/$C_3H_7NH_3^+$/$NH_3^+C_2H_4NH_3^+$) Aluminum Diphosphonates

Howard G. Harvey,[†] Simon J. Teat,[‡] Chiu C. Tang,[‡] Lachlan M. Cranswick,[§] and Martin P. Attfield*[,†,§]

Davy-Faraday Research Laboratory, The Royal Institution of Great Britain, 21 Albemarle Street, London W1S 4BS, U.K., CLRC Daresbury Laboratory, Daresbury, Warrington, Cheshire WA4 4AD, U.K., and School of Crystallography, Birkbeck College, Malet Street, Bloomsbury, London WC1E 7HX, U.K.

Received October 25, 2002

Three new aluminum diphosphonates ($C_3H_7NH_3$){AlF[(HO)$O_2PC_2H_4PO_3$]} (**1**) (orthorhombic, *Pnma*, $a = 8.2048(1)$ Å, $b = 6.90056(6)$ Å, $c = 19.6598(4)$ Å, $Z = 4$), ($H_3NC_2H_4NH_3$)[Al(OH)($O_3PC_2H_4PO_3$)] (**2**) (monoclinic, $P2_1/n$, $a = 11.142(3)$ Å, $b = 7.008(2)$ Å, $c = 12.903(5)$ Å, $\beta = 96.24(7)°$, $Z = 4$), and $(NH_4)_2$[AlF($O_3PCH_2PO_3$)] (**3**) (orthorhombic, *Cmcm*, $a = 16.592(2)$ Å, $b = 7.5106(9)$ Å, $c = 7.0021(9)$ Å, $Z = 4$) have been synthesized by solvothermal methods in the presence of linear organic ammonium cations (for **1** and **2)** and ammonium cations (for **3**) and their structures determined using powder, microcrystal, and single-crystal X-ray diffraction data, respectively. All three materials contain a similar one-dimensional chain motif which is related to that found in the mineral Tancoite. This chain motif consists of corner-sharing octahedra (AlO_4F_2 for **1** and **3** and AlO_6 for **2**) linked together through the bridging CPO_3 tetrahedra of the diphosphonate groups. These chains are unusual in that each diphosphonate moiety acts as a bisbidentate ligand that is coordinated to the same two metal centers through both of the O_3PC– groups of the diphosphonate ligand. The arrangement of the Tancoite-like chains and charge compensation cations in the structures of compounds **1**–**3** is seen to be dependent upon the nature of the diphosphonic acid and organoammonium/ammonium cations. Careful selection of these two components may provide a method to design future materials in this system.

Introduction

Research into the area of inorganic−organic hybrid materials has become a significant theme of materials chemistry over the last 15 years.[1−3] The attraction of these hybrid materials stems from the benefits introduced by inclusion of both inorganic and organic components into the product. In particular, the incorporation and modification of organic groups within structures allows the possibility of rationally designing materials with specific chemical properties and structures. Phosphonic acids [$RPO(OH)_2$, where R is an organic group] and diphosphonic acids [$(HO)_2OPRPO(OH)_2$] are excellent precursors for the preparation of such hybrid materials. Additional interest in metal phosphonate chemistry stems from potential application of these materials in areas such as, sorption,[4] ion-exchange,[5] sensing,[6,7] charge storage,[8] and catalysis.[9,10] Recent research has shown that diphosphonic acids are versatile building units for the synthesis of materials with extended architectures.[11] The diphosphonate group can be involved in structural connection, with the organic portion acting as a controllable spacer and the two inorganic groups chelating to the metal centers forming one,[12] two-,[13] and three-dimensionally extended structures.[14,15]

* To whom correspondence should be addressed. E-mail: m.attfield@mail.cryst.bbk.ac.uk. Tel: 00-44-20-7631-6813. Fax:: 00-44-20-7631-6803.
[†] The Royal Institution of Great Britain.
[‡] CLRC Daresbury Laboratory.
[§] Birkbeck College.

(1) Ferey, G. *Chem. Mater.* **2001**, *13*, 3084.
(2) Hagrman, P. J.; Hagrman, D.; Zubieta, J. *Angew. Chem., Int. Ed. Engl.* **1999**, *38*, 2639.
(3) Cheetham, A. K.; Ferey, G.; Loiseau, T. *Angew. Chem., Int. Ed. Engl.* **1999**, *38*, 3269.
(4) Maeda, K.; Kiyozumi, Y.; Mizukami, F. *J. Phys. Chem. B.* **1997**, *101*, 4402.
(5) Odobel, F.; Bujoli, B.; Massiot, D. *Chem. Mater.* **2001**, *13*, 163.
(6) Alberti, G.; Casciola, M.; Costantino, U.; Peraio, A.; Montoneri, E. *Solid State Ionics* **1992**, *50*, 315.
(7) Alberti, G.; Casciola, M. *Solid State Ionics* **1997**, *97*, 177.
(8) Vermeulen, L. A.; Thompson, M. E. *Nature* **1992**, *358*, 656.
(9) Deniaud, D.; Schollorn, B.; Mansuy, D.; Rouxel, J.; Battioni, P.; Bujoli, B. *Chem. Mater.* **1995**, *7*, 995.
(10) Maillet, C.; Janvier, P.; Pipelier, M.; Praveen, T.; Andres, Y.; Bujoli, B. *Chem. Mater.* **2001**, *13*, 2879.
(11) Clearfield, A. In *Progress in Inorganic Chemistry*; Karlin, K. D., Ed.; John Wiley & Sons: New York, 1998.

10.1021/ic020641q CCC: $25.00
Published on Web 03/12/2003

The structure adopted by metal diphosphonates is dependent upon many factors. For any particular metal species, two important factors include the specific diphosphonic acid used and the presence of any charge compensating cations occluded within the final structure. The diphosphonic acid can influence the final structure adopted through several means including the form of the organic spacer and the degree of protonation of the oxygen atoms of the phosphonate groups.[16−18] Similar factors apply to the occluded charge-compensating cationic species when considering its effect on the resultant structure adopted, such as the charge of the cation and its structure and relative hydrophobicity/hydrophilicity.[19−21] The charge-compensating cations may be inorganic or organic cations, as exemplified in microporous materials where the use of organic amines, as structure-directing agents, in the synthesis of new extended framework materials is well documented.[19] However, in the area of metal diphosphonate chemistry few examples are known in which organic amines are incorporated into the final material.

Currently, the only examples of amine-containing metal diphosphonates are those of the transition metal ions V,[16] Fe,[22] Cu,[23] and Zn[24] that are found to form zero- (mono- or dimeric), one-, two-, and three-dimensional extended structures. Surprisingly, the use of organic amine/ammonium species in the formation of aluminum phosphonates/diphosphonates has not been reported despite the routine use of such species to form new microporous aluminum phosphates. Most aluminum phosphonates/diphosphonates reported have neutral metal phosphonate extended structural components, for example, the two microporous phosphonate materials AlMePO-α and -β[25,26] and the pillared framework material $Al_2[O_3PC_2H_4PO_3](H_2O)_2F_2 \cdot H_2O$.[27] Exceptions to this trend include $Li_2Al_3[(HO)O_2P(CH_3)]_2[O_3P(CH_3)]_4Cl \cdot 7H_2O$, in which the charge of the cationic aluminum phosphonate layer is balanced by interlamellar Cl^- ions, and $Al(O_3P(CH_2)_3NH_3)SO_4 \cdot 3H_2O$, in which the cationic aluminum (aminopropyl)phosphonate chains are charge balanced by the anionic SO_4^{2-} groups.[28,29] However, no charge-compensating cation-containing aluminum disphosphonate materials have been reported in the literature.

Table 1. Initial Synthesis Gel Compositions, pH, and Product Formulas of Compounds **1**−**3**

$R(PO_3H_2)_2$:$Al_2(SO_4)_3 \cdot 18H_2O$:HF[a]:pyridine[b]:amine:H_2O; pH	formula
2.2:1:8.7:54.6:13.4:144; 7	$(C_3H_7NH_3)\{AlF[(HO)O_2PC_2H_4PO_3]\}$ (**1**)
2.2:1:8.7:1.1:36.2:144; 11.8	$(H_3NC_2H_4NH_3)[Al(OH)(O_3PC_2H_4PO_3)]$ (**2**)
2.2:1:8.7:54.6: 13.4:144; 5.8	$(NH_4)_2[AlF(O_3PCH_2PO_3)]$ (**3**)[c,d]

[a] HF/pyridine (70 wt % HF). [b] Includes pyridine from HF/pyridine. [c] Synthesis using tripropylamine resulted in **3** and an as yet unreported phase. [d] Synthesis using ammonium hydroxide resulted in **3** and an unidentified phase.

During the course of our program to prepare new diphosphonates of aluminum in the presence of charge-compensating cationic species we have discovered the three novel materials $(C_3H_7NH_3)\{AlF[(HO)O_2PC_2H_4PO_3]\}$ (**1**), $(H_3NC_2H_4NH_3)[Al(OH)(O_3PC_2H_4PO_3)]$ (**2**), and $(NH_4)_2[AlF(O_3PCH_2PO_3)]$ (**3**). These compounds represent the first aluminum diphosphonate materials to be synthesized in the presence of organic ammonium/ammonium species. All three materials contain aluminum diphosphonate chains that are related to those found in the mineral Tancoite, and compounds **1** and **2** provide the first examples of ethylenediphosphonate groups acting as bisbidentate ligands within this chain type.[30] The arrangement of these chains within the structure is seen to be dependent on the charge-compensating cationic species and the diphosphonate group itself and suggest that the resultant materials may be rationally designed by consideration of these factors.

Experimental Section

Materials and Methods. Compounds **1**−**3** were prepared by mixing together aluminum sulfate ($Al_2(SO_4)_3 \cdot 18H_2O$, Aldrich), ethylenediphosphonic acid (**1**, **2**) (Lancaster) or methylenediphosphonic acid (**3**) (Lancaster), HF/pyridine (70 wt % Aldrich), pyridine (Aldrich), and either propylamine (Aldrich) (**1**), ethylenediamine (Aldrich) (**2**), or NH_4OH (Aldrich) (**3**) and deionized water to form mixtures with the molar ratios and initial pH's summarized in Table 1. The reagent mixtures were loaded into 23 mL Teflon-lined steel autoclaves and heated for 4 days at 160 °C, under autogenous pressure. After being cooled and washed with distilled water and acetone, the crystalline products were separated by suction filtration.

Compound **1** was obtained as a polycrystalline powder, and compound **2** was obtained as microcrystals. Compound **3** was first synthesized with tripropylamine (Aldrich) added to the synthesis gel. This preparation resulted in the formation of single crystals of **3** which were used for the structure solution and another, as yet unreported, Al- and P-containing phase that can also be formed in the absence of an amine additive. We believe the ammonium cations

(12) Bonavia, G.; Haushalter, R. C.; O'Connor, C. J.; Zubieta, J. *Inorg. Chem.* **1996**, *35*, 5603.
(13) Gao, Q. M.; Guillou, N.; Nogues, M.; Cheetham, A. K.; Ferey, G. *Chem. Mater.* **1999**, *11*, 2937.
(14) Distler, A.; Lohse, D. L.; Sevov, S. C. *J. Chem. Soc., Dalton Trans.* **1999**, 1805.
(15) Poojary, D. M.; Zhang, B. L.; Clearfield, A. *J. Am. Chem. Soc.* **1997**, *119*, 12550.
(16) Soghomonian, V.; Chen, Q.; Haushalter, R. C.; Zubieta, J. *Angew. Chem., Int. Ed. Engl.* **1995**, *34*, 223.
(17) Poojary, D. M.; Zhang, B. L.; Bellinghausen, P.; Clearfield, A. *Inorg. Chem.* **1996**, *35*, 4942.
(18) Zapf, P. J.; Rose, D. J.; Haushalter, R. C.; Zubieta, J. *J. Solid State Chem.* **1996**, *125*, 182.
(19) Davis, M. E.; Lobo, R. F. *Chem. Mater.* **1992**, *4*, 756.
(20) Kubota, Y.; Helmkamp, M. M.; Zones, S. I.; Davis, M. E. *Microporous Mater.* **1996**, *6*, 213.
(21) Goretsky, A. V.; Beck, L. W.; Zones, S. I.; Davis, M. E. *Microporous Mesoporous Mater.* **1999**, *28*, 387.
(22) Zheng, L. M.; Song, H. H.; Lin, C. H.; Wang, S. L.; Hu, Z.; Yu, Z.; Xin, X. Q. *Inorg. Chem.* **1999**, *38*, 4618.
(23) Zheng, L. M.; Song, H. H.; Duan, C. Y.; Xin, X. Q. *Inorg. Chem.* **1999**, *38*, 5061.
(24) Song, H. H.; Zheng, L. M.; Wang, Z. M.; Yan, C. H.; Xin, X. Q. *Inorg. Chem.* **2001**, *40*, 5024.
(25) Maeda, K.; Kiyozumi, Y.; Mizukami, F. *Angew. Chem., Int. Ed. Engl.* **1994**, *33*, 2335.
(26) Maeda, K.; Akimoto, J.; Kiyozumi, Y.; Mizukami, F. *J. Chem. Soc., Chem. Commun.* **1995**, 1033.
(27) Harvey, H. G.; Teat, S. J.; Attfield, M. P. *J. Mater. Chem.* **2000**, *10*, 2632.
(28) Hix, G. B.; Wragg, D. S.; Bull, I.; Morris, R. E.; Wright, P. A. *J. Chem. Soc., Chem. Commun.* **1999**, 2421.
(29) Zakowsky, N.; Wheatley, P. S.; Bull, I.; Attfield, M. P.; Morris, R. E. *J. Chem. Soc., Dalton Trans.* **2001**, 2899.
(30) Hawthorne, F. C. *Tschermaks Mineral. Petrogr. Mitt.* **1983**, *31*, 121.

present in compound **3** are formed as a decomposition product of the tripropylamine under these synthesis conditions. This reaction was repeated using the conditions described above but in which tripropylamine was replaced by ammonium hydroxide. This resulted in the formation of **3** as a polycrystalline powder in addition to another unidentified Al- and F-containing polycrystalline phase.

Microprobe, EDXA, measurements were made using an Oxford Instrument ISIS system (EDS) fitted with a JEOL 773 Super-probe operating with an accelerating voltage of 15 kV and a beam diameter of 2 μm, under a vacuum of 10^{-12} Torr. Analysis of separate regions of the samples gave quantative results for Al:P ratios and qualitative results for fluorine.

Thermogravimetric analysis (TGA) data were collected using a Shimadzu TGA 50 thermogravimetric analyzer with the samples heated in open alumina crucibles under flowing nitrogen from 25 to 900 °C at a heating rate of 5 °C min^{-1}.

Magic angle spinning solid-state nuclear magnetic resonance (MAS SS NMR) data were recorded using a Bruker MSL 300 spectrometer. Spectra collected for ^{31}P nuclei were referenced to an 85% solution of H_3PO_4 with the spectrometer operating at a frequency of 121.49 MHz, a sample spinning speed of 6.3 kHz, and recycle delays of 10 s. For ^{19}F nuclei a $CFCl_3$ reference was used with a spectrometer operating frequency of 282.4 MHz, a sample spinning speed of 35 (**1**) and 20 (**3**) kHz, and a recycle delays of 5 s. Data collected for ^{15}N nuclei were referenced to $MeNO_3$ with a spectrometer operating frequency of 282.4 MHz, a sample spinning speed of 4.3 kHz, and recycle delays of 5 s.

Ab Initio Powder Structure Solution of Compound 1. The X-ray data used to determine the unit cell parameters of **1** were collected during a 12 h scan on a Siemens D500 X-ray diffractometer using Cu Kα_1 radiation (λ = 1.540 56 Å). The first 20 low-angle Bragg reflections were used to determine the orthorhombic unit cell parameters using the autoindexing program Treor-90 (figure of merit for indexing all 20 lines, $M(20) = 23.6$).[31] Synchrotron X-ray data were collected on a sample contained in a 0.5 mm diameter Lindemann glass capillary tube mounted on the high-resolution X-ray diffractometer at station 2.3, Daresbury SRS, Cheshire, U.K. The incident X-ray wavelength was 1.299 95 Å, selected using a Si(111) monochromator. The capillary tube was spun during data collection to minimize preferred orientation and sampling effects. Data were collected in steps of 0.01° in 2θ, with a collection time per step of 3 s between 6.5 and 20° 2θ, 6 s between 20 and 50° 2θ, 12 s between 50 and 80° 2θ, and 20 s between 80 and 84.51° 2θ. Corrections were made for synchrotron beam intensity decay through comparison with a beam flux monitor. Inspection of the synchrotron X-ray diffraction pattern revealed systematic absences consistent with the space group $P2_12_12_1$. One region of the diffraction data was excluded between 17.93 and 18.12° 2θ to remove a minor spurious peak not attributable to that of the structure being determined. Structure factors were extracted from this diffraction data by the Le Bail method[32] as implemented in the GSAS suite of programs.[33] The background of the diffraction profile for the Le Bail fit was fitted with a cosine Fourier series running through fixed points in the profile. The peak profiles were described by a pseudo-Voigt function with additional terms used to account for anisotropic particle size and strain broadening effects. The extracted structure factors were used in the direct methods program SIRPOW97,[34] via the EXPO interface,[35] to provide the Al, P, and some of the O and C atoms of the structure. This model was used as the starting model for the Rietveld refinement, again using the GSAS suite of programs.[33] The remaining atoms were located from difference Fourier maps. Inspection of the structure using the Addsym program, within the Platon suite of programs,[36] revealed that the structure may have the higher symmetry of *Pnma*. The structure was refined twice using each of the space groups following the same procedure. Initially, soft constraints were applied to all the Al−O/F, P−O/C, and C−C/N distances within the structure with the soft constraint weighting factor fixed at a high value. As the refinement progressed the soft constraint weighting factor was reduced to a final value of 3 in the latter cycles of the refinement. The final cycle of least-squares refinement included the background coefficients, peak profile parameters, a preferred orientation parameter, and positional and isotropic thermal parameters for all atoms in the structure. The thermal parameters of the P atoms and the O, F, C, and N atoms were constrained to have the same value during refinement. The Rietveld refinement gave reasonable bond lengths and angles and residuals in both symmetries (R_{wp} = 0.086, R_p = 0.070, and R_F = 0.080 for $P2_12_12_1$ and R_{wp} = 0.084, R_p = 0.072, and R_F = 0.079 for *Pnma*); however, the higher symmetry solution, *Pnma*, is reported as this fit was obtained using fewer refineable parameters. The crystallographic data and structure refinement parameters are given in Table 2, atomic coordinates and isotropic thermal factors are provided in the Supporting Information, and selected bond distances and angles are presented in Tables 3 and 4. The final observed, calculated and difference profiles are plotted in Figure 1, and the asymmetric unit is shown in Figure 2.

Table 2. Crystallographic Data and Structure Refinement Parameters for $(C_3H_7NH_3)AlF[(HO)O_2PC_2H_4PO_3]$ (**1**)

formula	$AlP_2FNO_6C_5H_{15}$
fw	277.954
temp (K)	293
wavelength (Å)	1.2999
space group	Pnma
a (Å)	8.2048(1)
b (Å)	6.90056(6)
c (Å)	19.6598(4)
V (Å^3)	1114.05(7)
Z	4
D_c (g cm^{-3})	1.657
R_p[a]	0.0718
R_{wp}[b]	0.0842
R_F[c]	0.0789

[a] $R_p = \Sigma|y_{io} - y_{ic}|/\Sigma y_{io}$. [b] $R_{wp} = \{\Sigma|w_i(y_{io} - y_{ic})^2|/\Sigma w_i y_{io}^2\}^{1/2}$. [c] $R_F = \Sigma||F_o| - |F_c||/\Sigma F_o|$.

Single-Crystal Structure Solutions of Compounds 2 and 3. Single-crystal X-ray data were collected from a single, colorless, needle-shaped microcrystal of compound **2** mounted on a Bruker AXS SMART CCD diffractometer at the high-flux single-crystal diffraction station 9.8 at CCLRC, Daresbury Laboratory Synchrotron Radiation Source, Cheshire, U.K., and from a single, colorless, prismatic crystal of compound **3** mounted on a Nonius Kappa CCD diffractometer with a Nonius FR591 rotating anode generator at the EPSRC national crystallography service, Southampton, U.K.. The structures of both compounds were solved by direct methods and refined by full-matrix least squares using the SHELX pro-

(31) Werner, P. E. *J. Appl. Crystallogr.* **1985**, *B41*, 418.
(32) Le Bail, A.; Duroy, H.; Fourquet, J. *Mater. Res. Bull.* **1988**, *23*, 447.
(33) Von Dreele, R. B.; Larson, A. C. *GSAS, General Structure Analysis System*; Regents of the University of California, LANSCE, Los Alamos National Laboratory: Los Alamos, NM, 1995.
(34) Altomare, A.; Burla, M. C.; Camalli, M.; Cascarano, G.; Giacovazzo, C.; Guagliardi, A.; Moliterni, A. G. G.; Polidori, G.; Spagna, R. *SIRPOW97*; Istituto di Ricerca per lo Sviluppo di Metodologie Cristallografiche (IRMEC): Bari, Italy, 1997.
(35) Altomare, A.; Burla, M. C.; Camalli, M.; Carrozzini, B.; Cascarano, G.; Giacovazzo, C.; Guagliardi, A.; Moliterni, A. G. G.; Polidori, G.; Rizzi, R. *J. Appl. Crystallogr.* **1999**, *32*, 339.
(36) Spek, A. L. *PLATON*; Utrecht University: Utrecht, Netherlands, 2001.

Table 3. Selected Bond Distances (Å) and Angles (deg) for **1**[a]

Al(1)−F(1)	1.841(2)	Al(1)−F(1)[a]	1.841(2)
Al(1)−O(1)	1.875(4)	Al(1)−O(1)[a]	1.875(4)
Al(1)−O(3)[b]	1.915(4)	Al(1)−O(3)[c]	1.915(4)
P(1)−O(1)	1.489(4)	P(1)−O(1)[b]	1.489(4)
P(1)−O(2)	1.568(7)	P(1)−C(1)[d]	1.799(8)
P(2)−O(3)	1.529(4)	P(2)−O(3)[b]	1.529(4)
P(2)−O(4)	1.557(6)	P(2)−C(2)	1.743(8)
C(1)−C(2)[d]	1.527(9)	C(3)−C(4)[d]	1.505(9)
C(3)−C(5)	1.521(9)	C(4)−N(1)	1.487(9)
F(1)−Al(1)−F(1)[a]	180.0	F(1)−Al(1)−O(1)	88.5(2)
F(1)−Al(1)−O(1)[a]	91.5(2)	F(1)−Al(1)−O(3)[b]	88.6(2)
F(1)−Al(1)−O(3)[c]	91.4(2)	F(1)[a]−Al(1)−O(1)	91.52(2)
F(1)[a]−Al(1)−O(1)[a]	88.5(2)	F(1)[a]−Al(1)−O(3)[b]	91.4(2)
F(1)[a]−Al(1)−O(3)[c]	88.6(2)	O(1)−Al(1)−O(1)[a]	180.0
O(1)−Al(1)−O(3)[b]	91.9(2)	O(1)−Al(1)−O(3)[c]	88.2(2)
O(1)[a]−Al(1)−O(3)[b]	88.2(2)	O(1)[a]−Al(1)−O(3)[c]	91.9(2)
O(3)[b]−Al(1)−O(3)[c]	180.0		
O(1)−P(1)−O(1)[b]	108.5(5)	O(1)−P(1)−O(2)	112.4(3)
O(1)−P(1)−C(1)[d]	112.7(4)	O(1)[b]−P(1)−O(2)	112.41(3)
O(1)[b]−P(1)−C(1)[d]	112.7(4)	O(2)−P(1)−C(1)[d]	98.0(5)
O(3)−P(2)−O(3)[b]	108.5(5)	O(3)−P(2)−O(4)	105.2(3)
O(3)−P(2)−C(2)	111.0(3)	O(3)[b]−P(2)−O(4)	105.2(3)
O(3)[b]−P(2)−C(2)	111.0(3)	O(4)−P(2)−C(2)	115.5(6)
C(4)[d]−C(3)−C(5)	106.3(9)	C(3)[d]−C(4)−N(1)	107.6(9)

[a] Symmetry transformations used to generate equivalent atoms: a, $-x$, $-y+1$, z; b, x, $y+1/2$, z; c, $-x$, $-y+3/2$, $-z$; d, $-x$, $-y+1$, $-z+1$.

Table 4. Hydrogen Bond Donor−Acceptor Distances (Å) for Compound **1**

donor···acceptor	D···A	donor···acceptor	D···A
O(2)···O(4)	2.616(5)	N(1)···O(3) × 2	2.862(7)
N(1)···O(4)	2.70(1)	N(1)···F(1)	3.32(1)

grams.[37,38] The thermal parameters of all of the non-hydrogen atoms were refined anisotropically. All the hydrogen atoms were found from difference Fourier maps and their thermal parameters refined isotropically. The bond length of the O−H bond in compound **2** was restrained in the structure refinement. The crystallographic data and structure refinement parameters for compounds **2** and **3** are given in Table 5, atomic coordinates and equivalent isotropic thermal factors are provided in the Supporting Information, and selected bond distances and angles are presented in Tables 6−9. The asymmetric units of compound **2** and **3** are shown in Figures 3 and 4, respectively.

Results

Structural Description of $(C_3H_7NH_3)\{AlF[(HO)O_2PC_2H_4PO_3]\}$ (1). The structure of $(C_3H_7NH_3)\{AlF[(HO)O_2PC_2H_4PO_3]\}$ (**1**) is shown in Figure 5. The main structural feature of **1** is the infinite anionic $[AlF(O_3PCH_2CH_2PO_3)]^{2-}{}_\infty$ chain running along the [010] direction. These chains comprise AlO_4F_2 octahedra sharing trans vertexes to form an infinite AlO_4F chain. The shared vertex was assigned as a fluorine atom [F(1)] in the structure determination, by analogy with the recently reported aluminum diphosphonate synthesized in the presence of HF.[27] Further evidence supporting the assignation of the shared vertex as a fluorine atom was provided by the EDXA measurements and the presence of a singlet at −144.2 ppm in the ^{19}F MAS SS NMR of the material (see Supporting Information), which confirmed the presence of one crystallographically independent fluorine site. The observed chemical shift is similar to that found for other bridging fluorine atoms found in aluminum-centered octahedra.[27,39] The average Al−O bond distance of 1.895 Å agrees well with those reported for Al in octahedral environments in other aluminophosphates and aluminophosphonates.[40,41] The average Al−F distance of 1.841 Å is consistent with those given for fluoraluminophosphates and phosphonates.[27,39]

The diphosphonate groups provide the oxygen atoms of the AlO_4F_2 octahedra. Adjacent AlO_4F_2 octahedra are bridged by a diphosphonate group, via the sharing of two of the oxygens of each of the constituent $-PO_3$ groups of the same diphosphonate ligand, to form the $[AlF(O_3PCH_2CH_2PO_3)]^{2-}{}_\infty$ chain, as shown in Figure 6a. The diphosphonate units bridge adjacent AlO_4F_2 octahedra on alternating sides along the $[AlF(O_3PCH_2CH_2PO_3)]^{2-}{}_\infty$ chains as seen in Figure 6a. The diphosphonate group is effectively acting as a bisbidentate ligand, a configuration that has not previously been observed in ethylenediphosphonate compounds. The tetrahedral PO_3C units display average P−O distances of 1.527 Å and average P−C distances of 1.771 Å, values typically found in other aluminum phosphonates and diphosphonates.[25,27,39] The ^{31}P MAS SS NMR spectrum of the material (see Supporting Information) shows two resonances, one at 23.27 and another at 14.52 ppm. This result is consistent with the two crystallographically independent phosphorus sites expected, and the chemical shift values are similar to those observed in other aluminum phosphonates.[4,42]

The $[AlF(O_3PCH_2CH_2PO_3)]^{2-}{}_\infty$ chains are similar in structure to those found in the mineral Tancoite, $LiNa_2H[Al(OH)(PO_4)_2]$,[30] and in other related minerals, where the chain has the general formula $[M\phi(TO_4)_2]$ (ϕ is an unspecified ligand).[30] One of the remaining oxygen atoms [O(2) or O(4)] of the PO_3 groups of each diphosphonate ligand, not involved in bonding in the AlO_4F_2 octahedra, is protonated, thus producing the complete formula of the constituent chains as $\{AlF[(HO)O_2PCH_2CH_2PO_3]\}^-{}_\infty$. This allows the $\{AlF[(HO)O_2PCH_2CH_2PO_3]\}^-{}_\infty$ chains to link together via interchain hydrogen bonding involving the O(2) and O(4) atoms to form layers in the *ab* plane as shown in Figure 5. The O(2)···O(4) distance between adjacent chains is 2.616(5) Å, a value similar to those reported for hydrogen-bonding distances observed in other metal diphosphonates.[13]

The layers formed in the *ab* plane contain "pockets" in which the propylammonium cations reside, as shown in Figure 7. The ^{15}N MAS SS NMR spectrum of the material (see Supporting Information) shows a peak with a chemical shift value of −347.2 ppm which lies within the expected range for protonated primary amines implying that the propylamine is present as the propylammonium cation in the

(37) Sheldrick, G. M. *SHELXS-86, A Program for Crystal Structure Determination*; University of Göttingen: Göttingen, Germany, 1986.
(38) Sheldrick, G. M. *SHELXL-97, A Program for Crystal Structure Determination*; University of Göttingen: Göttingen, Germany, 1997.
(39) Simon, N.; Guillou, N.; Loiseau, T.; Taulelle, F.; Ferey, G. *J. Solid State Chem.* **1999**, *147*, 92.
(40) Chippindale, A. M.; Turner, C. *J. Solid State Chem.* **1997**, *128*, 318.
(41) Maeda, K.; Akimoto, J.; Kiyozumi, Y.; Mizukami, F. *Angew. Chem., Int. Ed. Engl.* **1995**, *34*, 1199.
(42) Cabeza, A.; Aranda, M. A. G.; Bruque, S.; Poojary, D. M.; Clearfield, A.; Sanz, J. *Inorg. Chem.* **1998**, *37*, 4168.

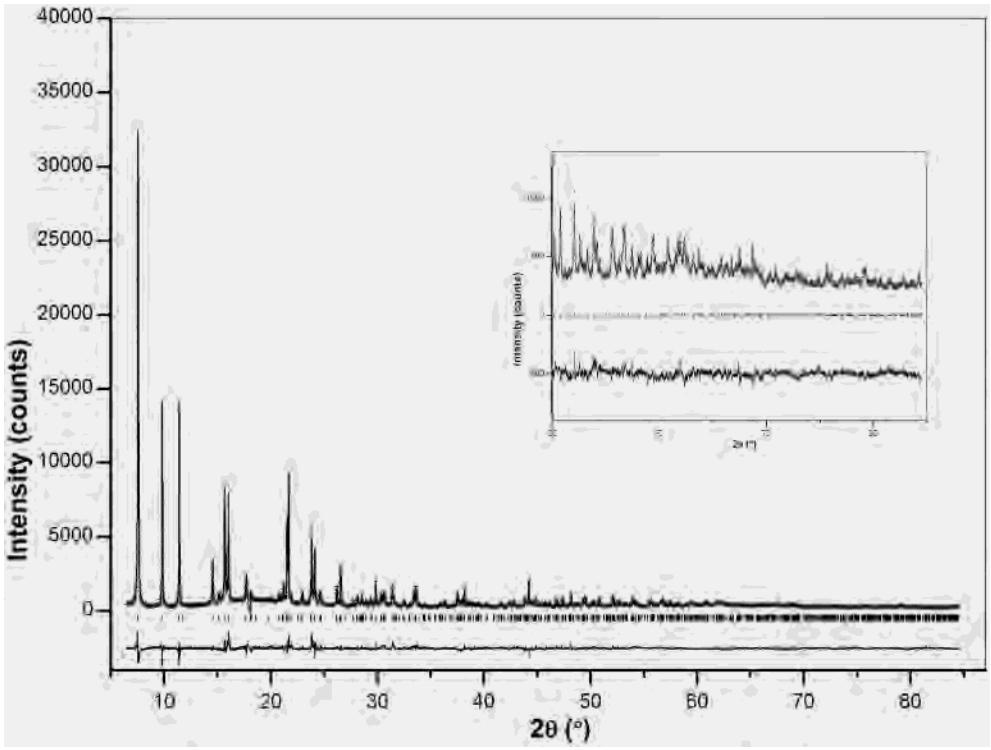

Figure 1. Final observed (crosses), calculated (solid), and difference profiles for the Rietveld refinement of $(C_3H_7NH_3)\{AlF[(HO)O_2PC_2H_4PO_3]\}$ (**1**). Reflection positions are shown as tick marks. The high-angle portion of the pattern is magnified for clarity.

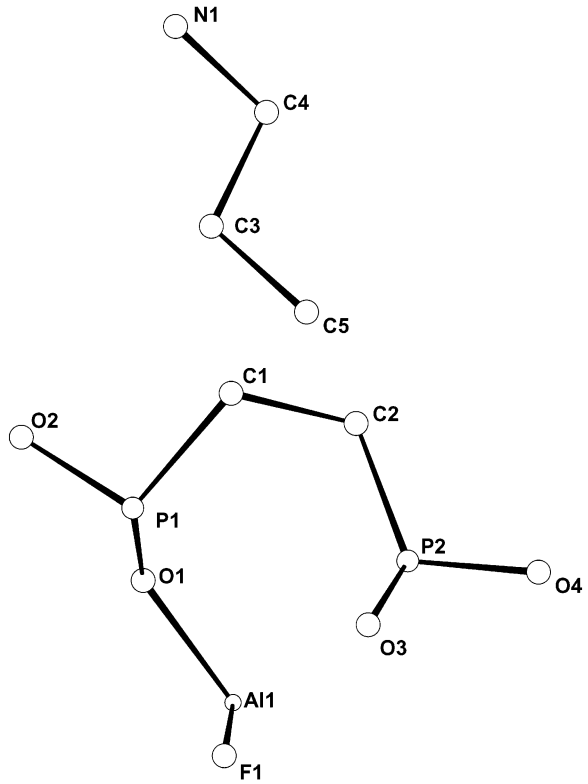

Figure 2. Asymmetric unit of $(C_3H_7NH_3)\{AlF[(HO)O_2PC_2H_4PO_3]\}$ (**1**).

structure.[43] The chain direction of the propylammonium cations is aligned perpendicular to the layers, along the [001] direction. The nitrogen atom N(1) of the propylammonium cations is held in the "pocket" by electrostatic interactions and hydrogen bonds to the oxygen and fluorine atoms of the $[AlF\{(HO)O_2PCH_2CH_2PO_3\}]^-_\infty$ chains (as indicated by the distances given in Table 4) with the organic tail of the propylammonium cation stretching out of the layer, as shown in Figures 5 and 7.

Table 5. Crystal Data and Structure Refinement Parameters for $(H_3NC_2H_4NH_3)[Al(OH)(O_3PC_2H_4PO_3)]$ (**2**) and $(NH_4)_2[AlF(O_3PCH_2PO_3)]$ (**3**)

formula	$AlP_2O_7NC_4H_{11}$	$AlP_2FO_6N_2CH_{10}$
fw	292.1	260.1
temp (K)	150	153
wavelength (Å)	0.689 30	0.710 73
space group	$P2_1/n$	Cmcm
a (Å)	11.142(3)	16.592(2)
b (Å)	7.008(2)	7.5106(9)
c (Å)	12.903(5)	7.0021(9)
β (deg)	96.24(7)	
V (Å^3)	1001.5(4)	872.6(1)
Z	4	4
D_c (g cm^{-3})	1.937	1.934
μ (mm^{-1})	0.432	0.620
R1 [$I > 2\sigma(I)$], R1 (all data)[a]	0.0526, 0.0920	0.0362, 0.0655
wR2 [I > 2σ(I)], wR2 (all data)[b]	0.1116, 0.1260	0.0774, 0.0939

[a] $R1 = \sum||F_o| - F_c||/\sum|F_o|$. [b] $wR2 = \{\sum[w(F_o^2 - F_c^2)^2]/\sum[w(F_o^2)^2]\}^{1/2}$ with $w = 1/[\sigma^2(F_o^2) + (aP)^2 + bP]$, where P is $[2F_c^2 + \mathrm{Max}(F_o^2,0)]/3$.

The propylammonium cation/Tancoite-like chain composite layers are stacked together in the [001] direction to complete the structure as depicted in Figure 5. These composite layers are held together through weaker van der Waals forces as their outer surface in the *ab* plane consists of alkyl groups from the diphosphonate and propylammonium groups only.

Structural Description of $(H_3NC_2H_4NH_3)[Al(OH)(O_3PC_2H_4PO_3)]$ (2). The structure of $(H_3NC_2H_4NH_3)[Al-$

(43) *Encyclopedia of Nuclear Magnetic Resonance*; Grant, D. M., Harris, R. K., Eds.; Wiley: Chichester, U.K., 1996.

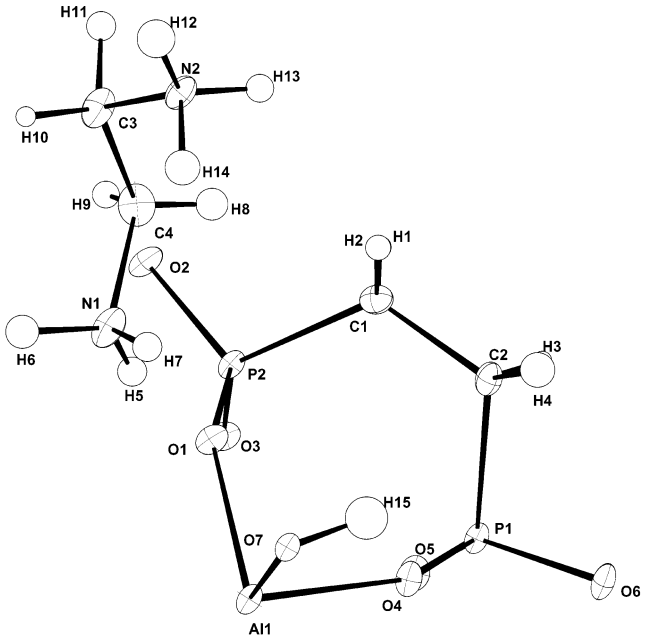

Figure 3. Asymmetric unit of $(H_3NC_2H_4NH_3)[Al(OH)(O_3PC_2H_4PO_3)]$ (**2**). Thermal ellipsoids are shown at 50% probability.

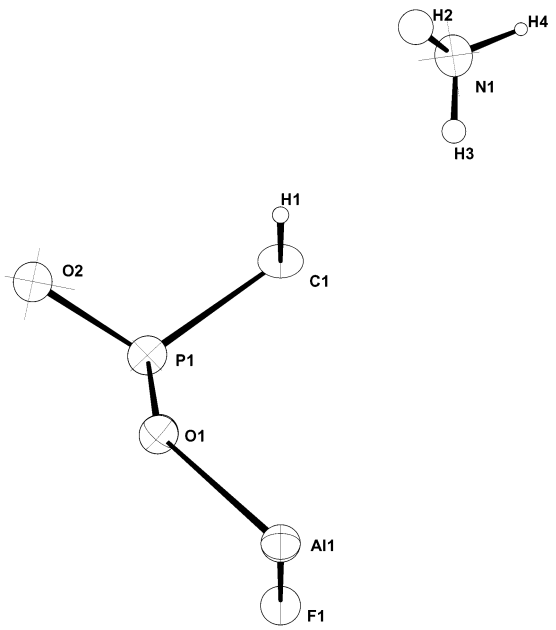

Figure 4. Asymmetric unit of $(NH_4)_2[AlF(O_3PCH_2PO_3)]$ (**3**). Thermal ellipsoids are shown at 50% probability.

$(OH)(O_3PC_2H_4PO_3)]$ (**2**) is shown in Figure 8. The main constituent of the structure is, again, the Tancoite-like infinite anionic $[Al(OH)(O_3PCH_2CH_2PO_3)]^{2-}_\infty$ chain running along the [010] direction, as shown in Figure 6b. The major differences of the Tancoite-like chain in **2** compared with that found in **1** is that the trans bridging fluorine atoms in **1** are replaced by trans bridging hydroxyl groups and the unbound diphosphonate oxygen atoms of the chain are unprotonated. The absence of fluorine signals in the EDXA and ^{19}F MAS SS NMR spectra of compound **2** and the presence of a hydrogen atom in the vicinity of O(7), found from difference Fourier maps, support the assignment of a bridging hydroxyl group in compound **2**. The average Al−O bond distance of 1.895 Å, average P−O distance of 1.524 Å, and average P−C distance of 1.808 Å all agree well with those reported for other aluminum phosphates, phosphonates, and diphosphonates.[25,27,39−41]

The ethylenediamine introduced into the synthesis gel of compound **2** is incorporated into the product as the diprotonated cation, all the hydrogen atoms of which have been located from difference Fourier maps. The diprotonated amine and the unprotonated Tancoite-like chains in **2** produce a different arrangement of these species in space with respect to the protonated amine and Tancoite-like chains observed in **1**, as shown in Figure 8. The structure of **2** consists of layers of alternating $[Al(OH)(O_3PCH_2CH_2PO_3)]^{2-}_\infty$ chains and ethylenediammonium cations. Each dication has significant hydrogen-bonding interactions with three independent anionic $[Al(OH)(O_3PCH_2CH_2PO_3)]^{2-}_\infty$ chains, in addition to electrostatic interactions between the aforementioned species, as indicated by the distances in Table 7. The unbound unprotonated diphosphonate oxygen atoms [O(2) and O(6)] form the shortest and, thus, strongest hydrogen bonds to the diprotonated ethylenediamine (see Table 7). Weaker van der Waals interactions exist between the organic part of the $[Al(OH)(O_3PCH_2CH_2PO_3)]^{2-}_\infty$ chains between layers.

Structural Description of $(NH_4)_2[AlF(O_3PCH_2PO_3)]$ (3). The structure of $(NH_4)_2[AlF(O_3PCH_2PO_3)]$ (**3**) is shown in Figure 9. The main constituent of the structure is, again, a Tancoite-like infinite anionic $[AlF(O_3PCH_2PO_3)]^{2-}_\infty$ chain running along the [001] direction, as shown in Figure 6c. This Tancoite-like chain contains trans bridging fluorine atoms linking the AlO_4F_2 octahedra, as in **1**, and the unbound diphosphonate oxygen atoms are deprotonated, as in **2**. The major difference between the Tancoite-like chain of **3** and those in **1** and **2** is the inclusion of the methylenediphosphonate group. The average Al−O bond distance of 1.874 Å, average Al−F bond distance of 1.880 Å, average P−O distance of 1.525 Å, and average P−C distance of 1.802 Å all agree well with those reported for other aluminum phosphates, phosphonates, and diphosphonates.[25,27,39−41]

The structure of **3** can be considered as consisting of layers of $[AlF(O_3PCH_2PO_3)]^{2-}_\infty$ chains interleaved by layers of inorganic ammonium cations in the *bc* plane as seen in Figure 9. Each NH_4^+ cation has significant hydrogen-bonding interactions with three different anionic $[AlF(O_3PCH_2PO_3)]^{2-}_\infty$ chains, in addition to electrostatic interactions, as indicated by the hydrogen-bond distances in Table 9. Weaker van der Waals interactions exist between the methylene groups of the $[AlF(O_3PCH_2PO_3)]^{2-}_\infty$ chains within a layer of Tancoite-like chains.

As mentioned previously, the structure of **3** was determined from a single crystal produced using tripropylamine in the synthesis gel. Subsequent synthesis, substituting tripropylamine for ammonium hydroxide, resulted in the formation of **3** as the dominant phase in a polycrystalline mixture of powders. The X-ray powder pattern of this sample is shown in Figure 10a and is in agreement with that calculated using the single-crystal solution, shown in Figure 10b. The presence of an, as yet unidentified, additional phase

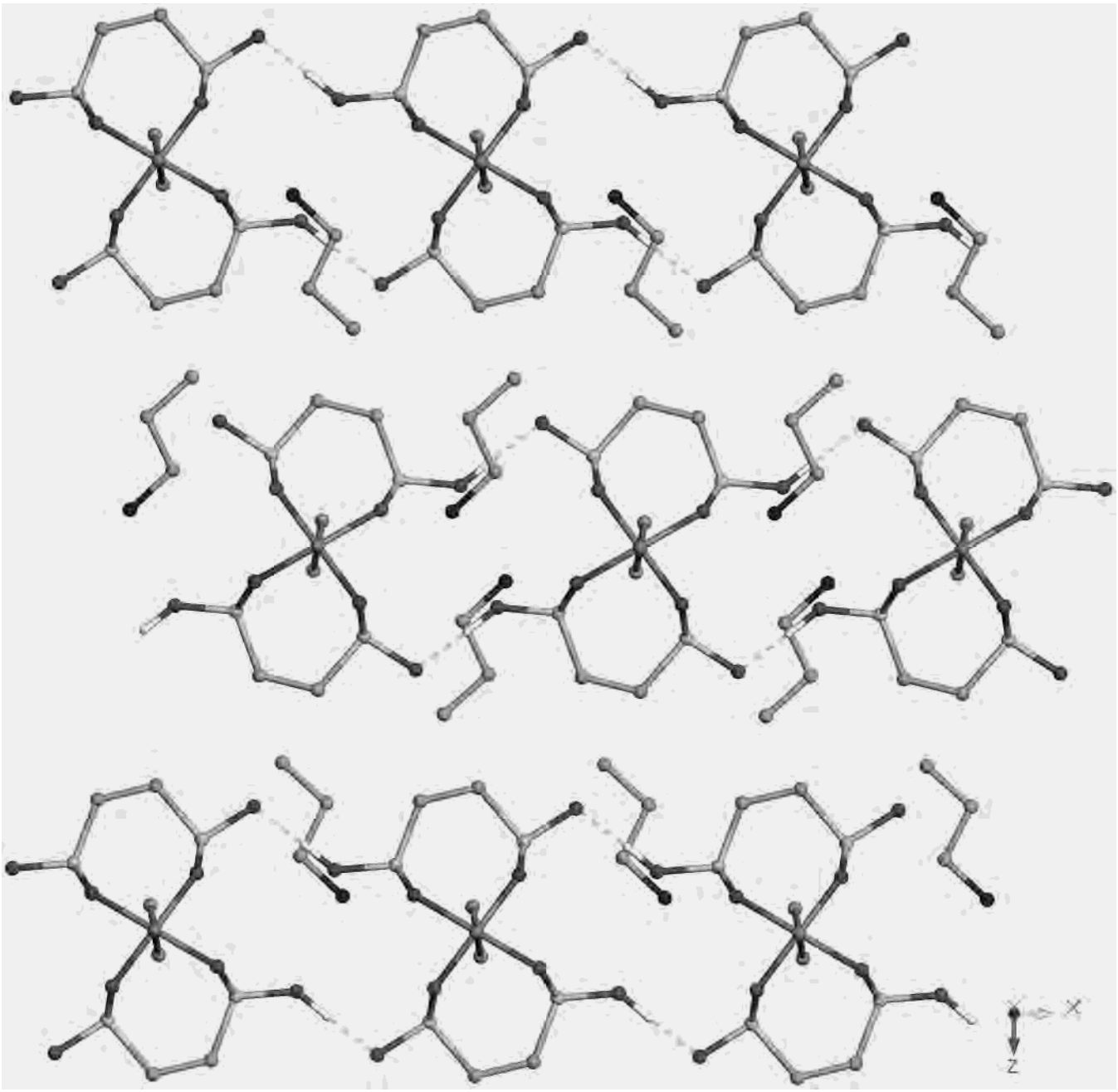

Figure 5. Structure of $(C_3H_7NH_3)\{AlF[(HO)O_2PC_2H_4PO_3]\}$ (**1**) viewed along the *y* axis. Hydrogen atoms have been assigned arbitrarily to the O(4) atoms of the O(2)···O(4) interacting pair of atoms, and the hydrogen bonds are represented by dotted lines.

is evidenced in the observed pattern by the presence of peaks at 17.18, 28.24, and 44.15° 2θ. Inspection of this sample using scanning electron microscopy revealed that the majority of the sample to be a powder with the composition of **3**. However, a small portion of the sample appears as larger subspherical particles ($\approx$40 μm), for which EDXA analysis reveals the presence of aluminum and fluorine but no phosphorus. The ^{19}F NMR of this polycrystalline sample (see Supporting Information) shows a dominant peak at −140.5 ppm which has a chemical shift of similar value to other bridging fluorine atoms found in aluminum-centered octahedra. An additional smaller peak is found centered at −149.04 ppm, which is assumed to be due to the non-phosphorus-containing impurity phase.

Thermal Analyses. The TGA traces for compounds **1**−**3** are shown in Figure 11. The trace for compound **1** displays a single mass loss between 190 and 490 °C of 31.02% that occurs most rapidly between 315 and 365 °C. This loss is assumed to be due to the combined mass loss of the propylamine and the ethylene component of the diphosphonate group (calculated 31.68%). The trace for compound **2** shows a small mass loss between 40 and 210 °C, a second mass loss of 22.4% between 210 and 450 °C, and a third smaller mass between 450 and 630 °C. These mass losses are attributed to surface dehydration, loss of one ethylenediamine molecule (calculated 21.1%), and decomposition of the organic portion of the ethylenediphosphonate group, respectively. The TGA trace of the polycrystalline sample

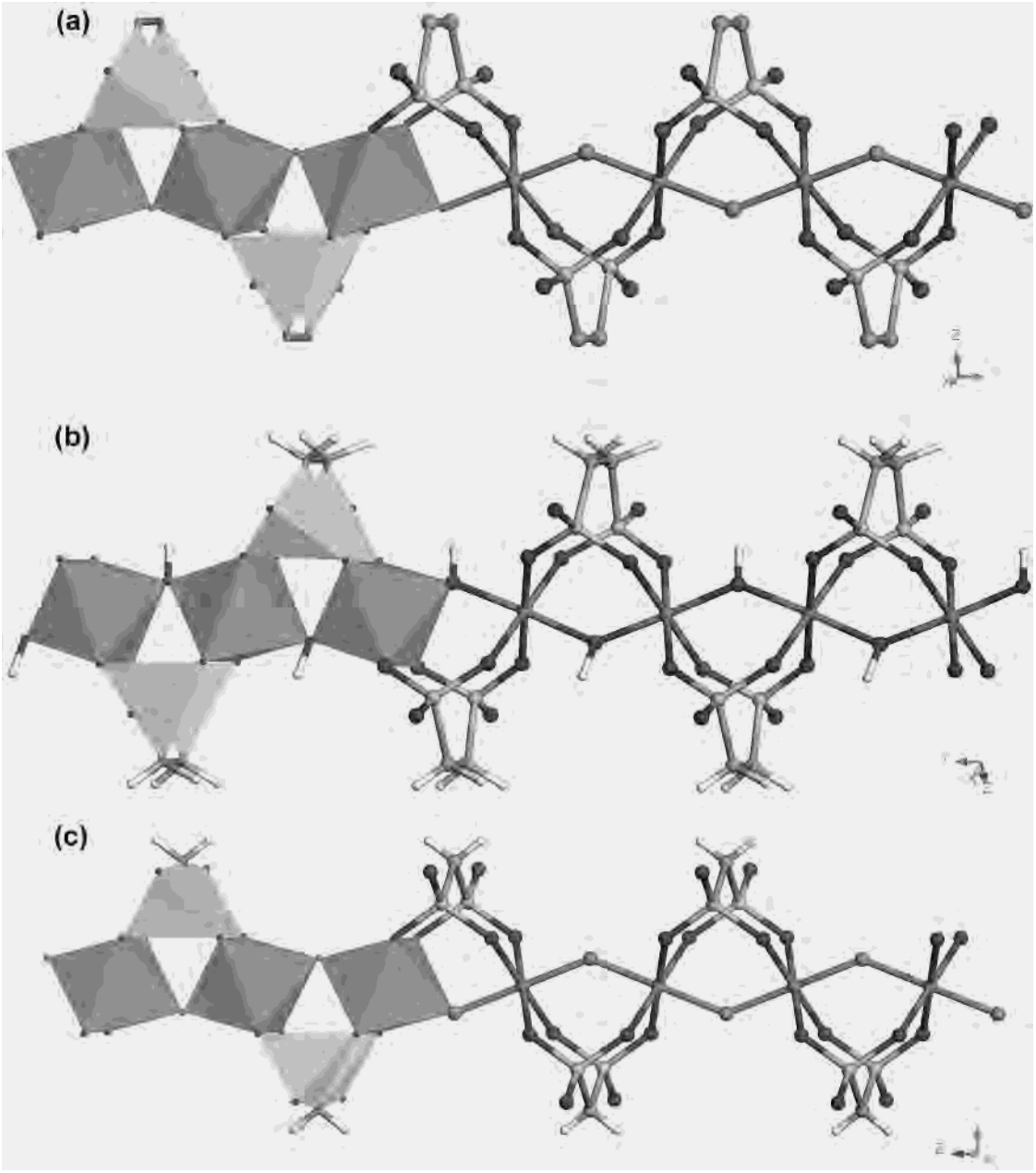

Figure 6. Structure of the Tancoite-like chains of compound **1** (a), **2** (b), and **3** (c) represented in polyhedral and ball-and-stick modes.

of compound **3** shows four separate mass losses. The mass loss for the first of these losses, between 160 and 260 °C, is assumed to be due to loss of the ammonium molecules, although further rationalization is limited due to the phase impurity of the sample.

Discussion

The preparation and structure of the three reported compounds containing similar Tancoite-like chains allows a comparison to be made between the use of different diphosphonic acids and charge-compensating cationic species in the preparation and design of such materials.

The synthetic conditions, see Table 1, used in the synthesis of **1** and **2** are similar, but the differences in the resulting structures stem from the added amines. Propylamine and ethylenediamine are both linear amines with chain lengths of 4 atoms but with different terminal groups, $-CH_3$ in the former and $-NH_2$ in the latter. Propylamine has a single Brønsted base site and has the ability to form a monoprotonated conjugate acid only. Formation of such a conjugate acid produces a species with a charged/hydrophilic end and a nonpolar/hydrophobic end. The effects of using such a primary alkylamine in the synthesis of compound **1** are evident in the resulting structure. Since the propylamine can only accept a single proton, a proton remains on the Tancoite-like $\{AlF[(HO)O_2PC_2H_4PO_3]\}^-_\infty$ chains for charge compensation. This results in these chains forming the hydrogen-bonded layers shown in Figure 5 with the polar/hydrophilic regions of the Tancoite-like chain interacting along the *a* axis perpendicular to the hydrophobic ethylene groups of

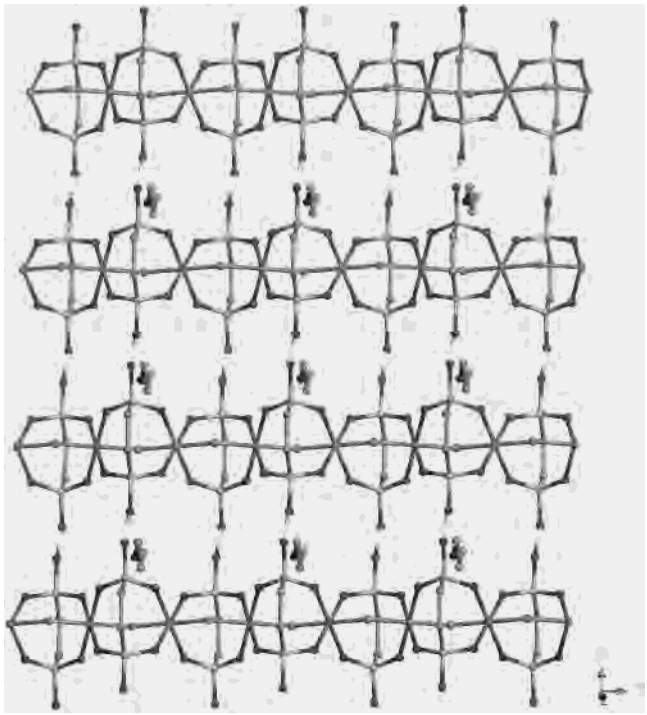

Figure 7. Structure of $(C_3H_7NH_3)\{AlF[(HO)O_2PC_2H_4PO_3]\}$ (**1**) viewed along the *z* axis. Hydrogen atoms have been assigned arbitrarily to the O(4) atoms of the O(2)···O(4) interacting pair of atoms, and the hydrogen bonds are represented by dotted lines.

the Tancoite-like chain that align along the *c* axis. The dual hydrophilic/hydrophobic nature of the propylammonium cation is reflected in the structure, with the charged $-NH_3^+$ group buried in the hydrophilic region of the hydrogen-bonded Tancoite-like chain layer and the nonpolar tail being directed toward the hydrophobic regions of the structure. This results in an overall layer type structure, in which each propylammonium cation/Tancoite-like chain composite layer is held together by strong intralayer electrostatic based forces

Table 6. Selected Bond Distances (Å) and Angles (deg) for **2**[a]

Al(1)−O(7)[a]	1.880(2)	Al(1)−O(4)	1.883(2)
Al(1)−O(5)[b]	1.888(3)	Al(1)−O(7)	1.891(2)
Al(1)−O(3)[b]	1.908(3)	Al(1)−O(1)	1.919(3)
P(1)−O(6)	1.517(2)	P(1)−O(5)	1.524(2)
P(1)−O(4)	1.529(2)	P(1)−C(2)	1.815(3)
P(2)−O(2)	1.519(2)	P(2)−O(1)	1.525(2)
P(2)−O(3)	1.529(2)	P(2)−C(1)	1.801(3)
C(2)−C(1)	1.556(5)		
N(1)−C(4)	1.498(5)	N(2)−C(3)	1.485(4)
C(3)−C(4)	1.506(5)		
O(7)[a]−Al(1)−O(4)	89.2(1)	O(7)[a]−Al(1)−O(5)[b]	91.2(1)
O(4)−Al(1)−O(5)[b]	179.0(1)	O(7)[a]−Al(1)−O(7)	177.62(8)
O(4)−Al(1)−O(7)	88.6(1)	O(5)[b]−Al(1)−O(7)	91.1(1)
O(7)[a]−Al(1)−O(3)[b]	90.0(1)	O(4)−Al(1)−O(3)[b]	89.9(1)
O(5)[b]−Al(1)−O(3)[b]	89.1(1)	O(7)−Al(1)−O(3)[b]	90.9(1)
O(7)[a]−Al(1)−O(1)	90.1(1)	O(4)−Al(1)−O(1)	92.0(1)
O(5)[b]−Al(1)−O(1)	88.9(1)	O(7)−Al(1)−O(1)	89.1(1)
O(3)[b]−Al(1)−O(1)	178.1(1)		
O(6)−P(1)−O(5)	111.8(1)	O(6)−P(1)−O(4)	110.9(1)
O(5)−P(1)−O(4)	112.1(1)	O(6)−P(1)−C(2)	104.5(1)
O(5)−P(1)−C(2)	109.8(1)	O(4)−P(1)−C(2)	107.2(1)
O(2)−P(2)−O(1)	111.7(1)	O(2)−P(2)−O(3)	109.4(1)
O(1)−P(2)−O(3)	112.6(1)	O(2)−P(2)−C(1)	105.7(1)
O(1)−P(2)−C(1)	108.5(2)	O(3)−P(2)−C(1)	108.7(1)
N(2)−C(3)−C(4)	112.1(3)	N(1)−C(4)−C(3)	115.1(3)

[a] Transformations used to generate symmetry-equivalent atoms: a, $-x + 3/2$, $y + 1/2$, $-z + 1/2$; b, $-x + 3/2$, $y - 1/2$, $-z + 1/2$.

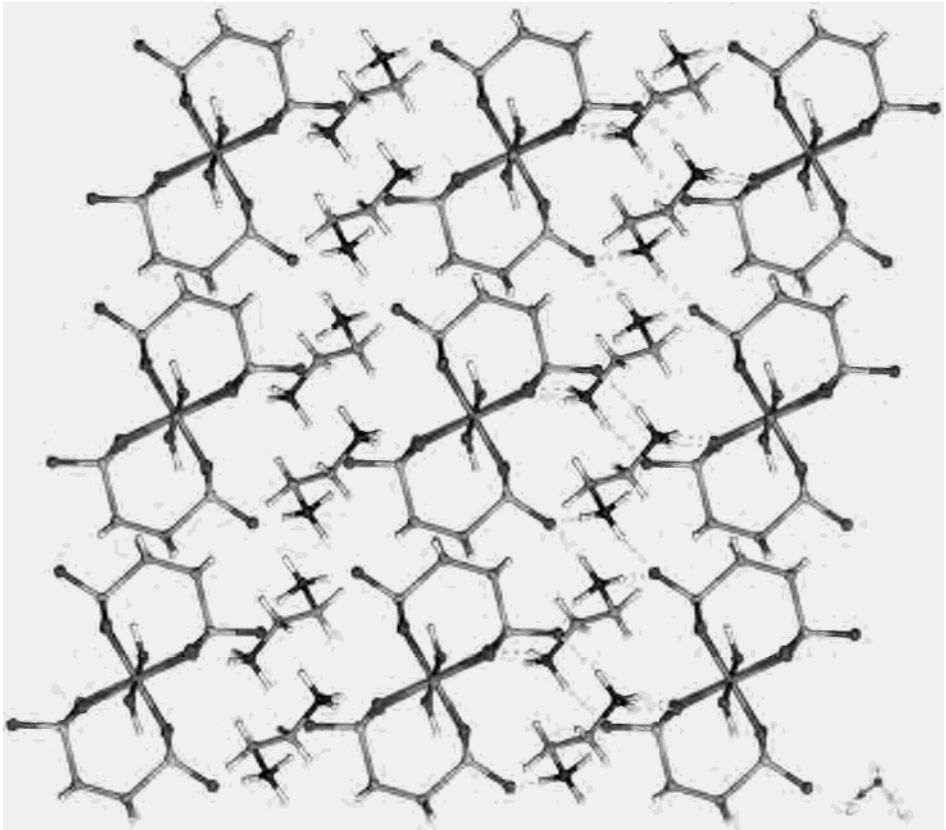

Figure 8. Structure of $(H_3NC_2H_4NH_3)[Al(OH)(O_3PC_2H_4PO_3)]$ (**2**) viewed along the *y* axis. Hydrogen bonds are represented by dotted lines.

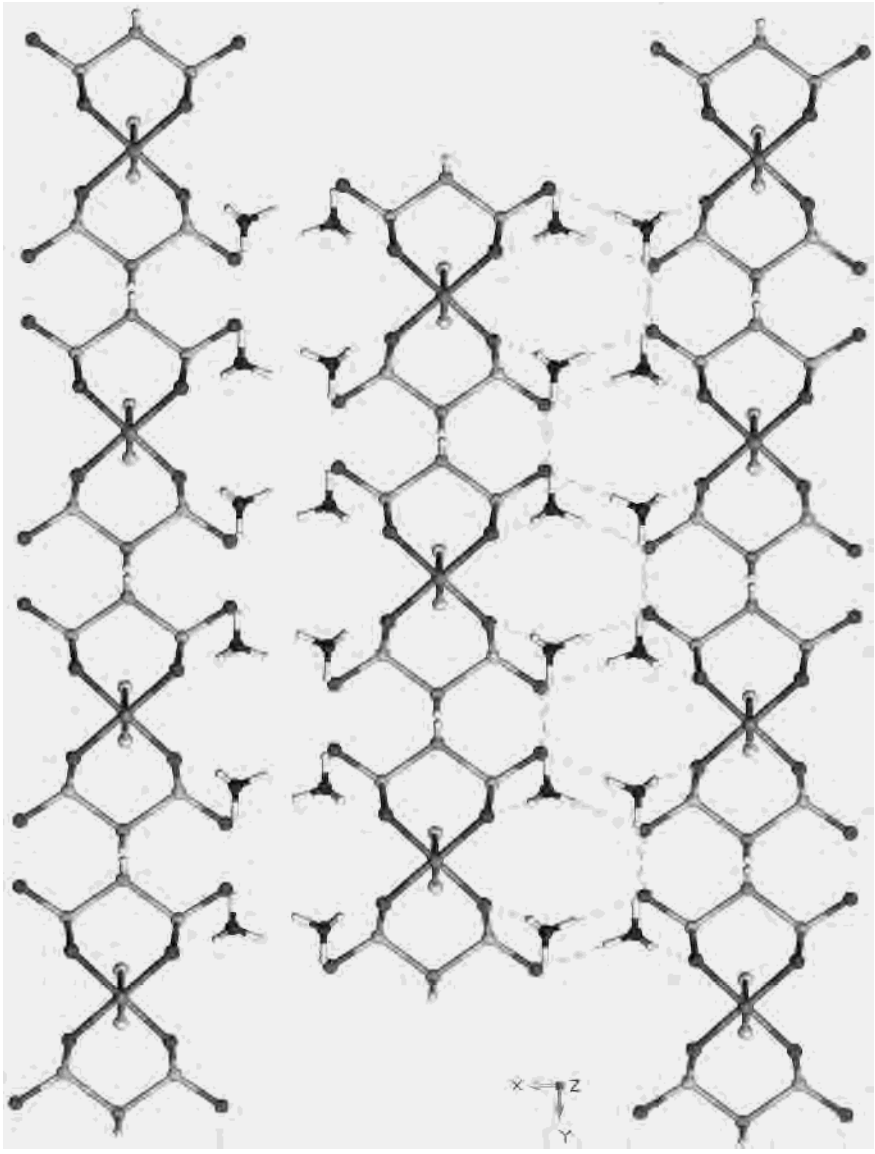

Figure 9. Structure of $(NH_4)_2[AlF(O_3PCH_2PO_3)]$ (**3**) viewed along the *z* axis. Hydrogen bonds are represented by dotted lines.

Table 7. Hydrogen Bond Distances (Å) and Angles (deg) for **2**

donor−H···acceptor	D−H	H···A	D···A	D−H···A
N(1)−H(5)···O(1)	0.87(5)	2.00(5)	2.852(4)	166(4)
N(1)−H(6)···O(2)	0.99(5)	1.75(4)	2.737(4)	169(4)
N(1)−H(7)···O(3)	0.94(5)	1.93(5)	2.837(4)	162(4)
N(2)−H(12)···O(6)	0.99(5)	1.74(5)	2.726(4)	173(5)
N(2)−H(13)···O(6)	0.95(4)	1.81(4)	2.738(4)	163(4)
N(2)−H(14)···O(2)	1.05(5)	1.66(5)	2.675(4)	160(4)

Table 8. Selected Bond Distances (Å) and Angles (deg) for **3**[a]

Al(1)−O(1)^b	1.874(1)	Al(1)−O(1)	1.874(1)
Al(1)−O(1)^c	1.874(1)	Al(1)−O(1)^d	1.874(1)
Al(1)−F(1)	1.880(1)	Al(1)−F(1)^b	1.880(1)
P(1)−O(2)	1.502(3)	P(1)−O(1)	1.537(1)
P(1)−O(1)^a	1.537(1)	P(1)−C(1)	1.802(3)
O(1)^b−Al(1)−O(1)	180.0(1)	O(1)^b−Al(1)−O(1)^c	88.3(1)
O(1)−Al(1)−O(1)^c	91.7(1)	O(1)^b−Al(1)−O(1)^d	91.7(1)
O(1)−Al(1)−O(1)^d	88.3(1)	O(1)^c−Al(1)−O(1)^d	180.00(6)
O(1)^b−Al(1)−F(1)	90.48(8)	O(1)−Al(1)−F(1)	89.52(8)
O(1)^b−Al(1)−F(1)^b	89.52(8)	O(1)^d−Al(1)−F(1)	90.48(8)
O(1)−Al(1)−F(1)^b	90.48(8)	O(1)^c−Al(1)−F(1)^b	90.48(8)
O(1)^d−Al(1)−F(1)^b	89.52(8)	F(1)−Al(1)−F(1)^b	180.0(1)
O(1)^c−Al(1)−F(1)	89.52(8)		
O(2)−P(1)−O(1)	112.07(8)	O(2)−P(1)−O(1)^a	112.07(8)
O(1)−P(1)−O(1)^a	110.1(1)	O(1)−P(1)−C(1)	105.1(1)
O(2)−P(1)−C(1)	111.9(1)	O(1)^a−P(1)−C(1)	105.1(1)
P(1)^c−C(1)−P(1)	109.3(3)		

[a] Symmetry transformations used to generate equivalent atoms: a, x, y, $-z + 1/2$; b, $-x$, $-y$, $-z$; c, $-x$, y, z; d, x, $-y$, $-z$; e, $-x$, $-y$, $z + 1/2$.

and weaker van der Waals forces exist between the layers. The resulting structure of **1** would be expected to cleave easily along the *ab* plane.

The ethylenediamine molecules used in the synthesis of **2** possess two Brønsted base sites. The two charged $-NH_3^+$ end groups of the diamine in the structure interact strongly with the polar/hydrophilic sections of the Tancoite-like $[Al(OH)(O_3PCH_2CH_2PO_3)]^{2-}_{\infty}$ chains, particularly the unprotonated O(2) and O(6) atoms, and result in the ethylenediammonium cations of the organoammonium cation/Tancoite-like chain composite layer of **2** (see Figure 8) being oriented perpendicular to the propylammonium cations found in the structure of the organoammonium cation/Tancoite-like chain composite layer of **1** (see Figure 5). The resultant effect of

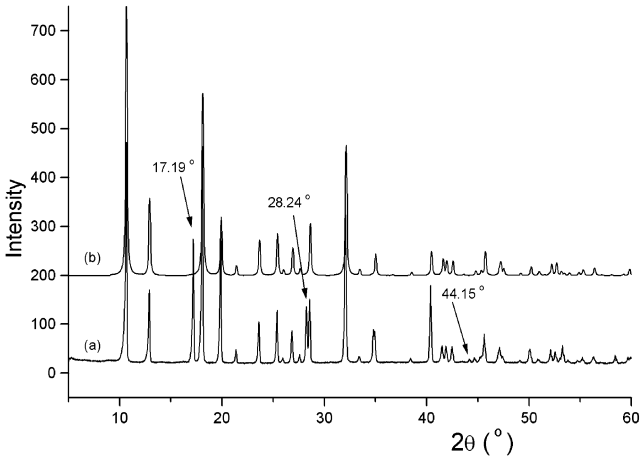

Figure 10. Observed X-ray powder diffraction pattern of the mixed-phase powder sample containing compound **3** (a) and the calculated pattern of compound **3** (b).

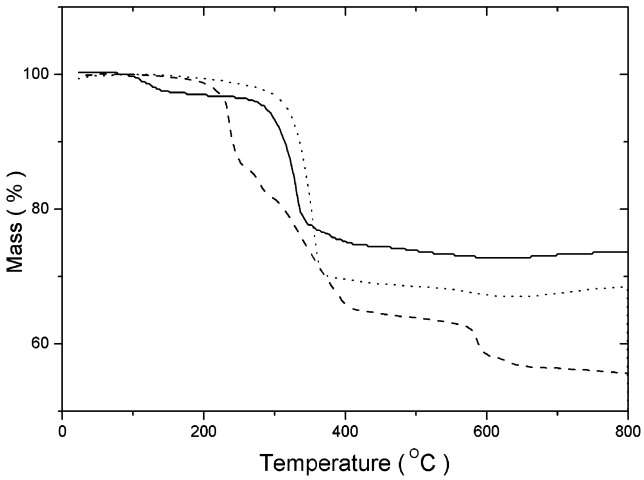

Figure 11. Thermogravimetric analysis traces of compound **1** (dots), **2** (solid), and **3** (dashes).

Table 9. Hydrogen Bond Distances (Å) and Angles (deg) for **3**

donor−H···acceptor	D−H	H···A	D···A	D−H···A
N(1)−H(2)···O(1)	0.92(3)	1.92(3)	2.831(3)	166(3)
N(1)−H(3)···O(2) × 2	0.83(5)	1.94(4)	2.771(4)	173(3)
N(1)−H(4)···O(2)	0.79(3)	2.01(3)	2.798(4)	179(4)

the differing nature of the occluded organoammonium cations in **1** and **2** is noticeable in the different stacking of the organoammonium cation/Tancoite-like chain composite layers within the structures. In structure **1** adjacent organoammonium cation/Tancoite-like chain composite layers are translated 1/2*a* in the [100] direction relative to each other (AB stacking), while in structure **2** the composite layers are aligned every eight layers (ABCDEFG stacking). The structure of **2** is strongly bound in all three dimensions by each ethylenediammonium cation interacting with three different Tancoite-like chains.

The use of the hydrophilic ammonium cations as the charge-compensating species in the formation of compound **3** produces another arrangement of the Tancoite-like chains. In compound **3** the unbound diphosphonate oxygen atoms of the Tancoite-like $[AlF(O_3PCH_2PO_3)]^{2-}_{\infty}$ chains are unprotonated, so these chains do not form a hydrogen-bonded layer as in compound **1**. The small size of the ammonium cations allows for two separate cations to be incorporated into the structure of **3** in the space occupied by one ethylenediammonium cation in the structure of compound **2**. However, the structure adopted by compound **3** is different from structures **1** and **2** in that the Tancoite-like chains in adjacent rows in the *ac* plane in **3** (see Figure 9) are unaligned, unlike the Tancoite-like chains in the *ab* plane (see Figure 5) and parallel to the (101) plane (see Figure 8) in structures **1** and **2**, respectively. Each ammonium cation hydrogen bonds to three different Tancoite-like chains making the structure strongly bound in all three-dimensions.

Another notable feature, evident in these three compounds, is the segregation of hydrophobic and hydrophilic portions of the Tancoite-like chains and charge-compensating species within the structure as shown in Figures 5, 8, and 9. This is most apparent in compound **1**, where the composite layers of the structure have a hydrophobic exterior, consisting of the ethylene portions of the diphosphonate ligands and the alkyl chain of the propylammonium cations, and a hydrophilic interior, composed of the $-NH_3^+$ group of propylammonium cations and the inorganic portion of the Tancoite-like chains. In compounds **2** and **3** the charge-compensating species are more polar; thus, there are larger hydrophilic regions within these compounds. The hydrophobic portions of the Tancoite-like chains in compounds **2** and **3** align to maximize their interactions. This segregation of hydrophobic and hydrophilic regions is a common feature of metal phosphonates and other hybrid materials and may be considered in the design of future materials.

These three compounds provide further examples of the preparation of Tancoite or Tancoite-like chains based on phosphorus-containing groups. The Tancoite chain, denoted $[M\phi(TO_4)_2]_n$, is a common motif in phosphate chemistry;[30] however, sulfate and silicate analogues are also known.[44,45] Aside from natural Tancoite (discovered at the Tanco Mine, Bernie Lake, Manitoba,[46]) structures containing this type of chain have been prepared synthetically using various metal-centered octahedra, including Al,[47,48] Ga,[49−52] Fe,[53,54] and V,[55] and various charge compensating cations, including organoammonium dications and metal and ammonium cations. It is now becoming apparent that the phosphate group in the

(44) Scodari, F. *Tschermaks Mineral. Petrogr. Mitt.* **1981**, *28*, 315.
(45) Balko, V. P.; Bakakin, V. V. *Zh. Strukt. Khim.* **1975**, *16*.
(46) Ramik, R. A.; Sturman, B. D.; Dunn, P. J.; Poverennykh, A. S. *Can. Mineral.* **1980**, *18*.
(47) Attfield, M. P.; Morris, R. E.; Burshtein, I.; Campana, C. F.; Cheetham, A. K. *J. Solid State Chem.* **1995**, *118*, 412.
(48) Lii, K. H.; Wang, S. L. *J. Solid State Chem.* **1997**, *128*, 21.
(49) Lin, H. M.; Lii, K. H. *Inorg. Chem.* **1998**, *37*, 4220.
(50) Walton, R. I.; Millange, F.; O'Hare, D.; Paulet, C.; Loiseau, T.; Ferey, G. *Chem. Mater.* **2000**, *12*, 1977.
(51) Walton, R. I.; Millange, F.; Le Bail, A.; Loiseau, T.; Serre, C.; O'Hare, D.; Ferey, G. *J. Chem. Soc., Chem. Commun.* **2000**, 203.
(52) Millange, F.; Walton, R. I.; Guillou, N.; Loiseau, T.; O'Hare, D.; Ferey, G. *J. Chem. Soc., Chem. Commun.* **2002**, 826.
(53) Lethbridge, Z. A. D.; Lightfoot, P.; Morris, R. E.; Wragg, D. S.; Wright, P. A.; Kvick, A.; Vaughan, G. *J. Solid State Chem.* **1999**, *142*, 455.
(54) Cavellec, M.; Riou, D.; Greneche, J. M.; Ferey, G. *Inorg. Chem.* **1997**, *36*, 2187.
(55) Zhang, Y. P.; Warren, C. J.; Clearfield, A.; Haushalter, R. C. *Polyhedron* **1998**, *17*, 2575.

Table 10. Nearest Neighbor P−P Distances (Å) in Tancoite/Tancoite-like Chains

P−P linkage	compd	dist
P−O−P	$(NH_3C_3H_6NH_3)[GaF(O_3POPO_3)]\cdot 3H_2O$[52]	2.851
P−CH_2−P	$(NH_4)_2[AlF(O_3PCH_2PO_3)]$	2.940
P−CH_2−CH_2−P	$(H_3NC_2H_4NH_3)[Al(OH)(O_3PC_2H_4PO_3)]$	3.401
P−O−H···O−P	$(NH_3C_3H_6NH_3)[GaF(HPO_4)_2]$[50]	3.705
none (P−O···O−P)	$Na_4[Al(OH)(PO_4)_2]$[47]	3.875

basic Tancoite chain can be replaced by other monomeric phosphorus-centered tetrahedral groups, for example, phosphite,[56] and dimeric groups, such as diphosphate[52] and methylenediphosphonate.[12,14] Compounds **1** and **2** extend this trend further and are the first examples of Tancoite-like chain structures that contain a longer alkyldiphosphonate group behaving in this bisbidentate fashion. There is an example of a structure containing Tancoite-like chains involving ethylenediphosphonate groups; however, each $-CPO_3$ tetrahedral unit of each ethylenediphosphonate group is bound to a different Tancoite-like chain, unlike compounds **1** and **2**.[57]

The paucity of structures containing Tancoite-like chains involving bisbidentate ethylenediphosphonate groups, compared to methylenediphosphonate groups, may be due to the unfavorable strain energy within the bound bisbidentate ligand. When methylenediphosphonate is the bisbidentate ligand, as in compound **3**, the observed P(1)−C(1)−P(1) angle has a value of 109.3(3)°, which is close to the expected ideal value for a tetrahedrally bound carbon atom. In compounds **1** and **2** the observed P−C−C angles are 116.8(8) and 124.3(8)° and 120.9(2) and 120.5(2)°, respectively. Both compounds contain P−C−C angles that deviate considerably from the ideal value for tetrahedrally bound carbon atoms.

Many Tancoite and Tancoite-like chains that contain phosphorus-centered tetrahedra and linked tetrahedra have now been reported. This implies that this system may have the potential to be subtly manipulated to rationally design structures containing specific Tancoite-like chains and for which the spatial arrangement of these chains may be determined through judicious choice of reagents, such as the nature and type of the charge-compensating cationic species, the octahedrally coordinated metal center, and the phosphorus-containing tetrahedral units. The fine control of structural aspects in this system is exemplified by the range of nearest-neighbor P−P distances, given in Table 10, that can be formed by the use of different phosphorus containing groups in the synthesis of these materials. Such structural control of the resultant materials is desirable to govern the properties, such as magnetic interactions,[12,14,54] within and between the Tancoite-like chains of these low-dimensional structures.

Acknowledgment. The authors thank Dr. A. Aliev and Dr. M. Odlyha of the ULIRS for collection of the SS MAS NMR and TGA data, respectively, and the EPSRC National Crystallography Service, University of Southampton, Southampton, U.K., for collecting single-crystal X-ray data for compound **3**. M.P.A. thanks the Royal Society for provision of a University Research Fellowship, and H.G.H. thanks the EPSRC for provision of a quota award and for funding.

Supporting Information Available: The ^{19}F, ^{31}P, and ^{15}N MAS SS NMR spectra of compound **1**, the ^{19}F MAS SS NMR spectrum of compound **3**, and the CIF files for compounds **1**−**3**. This material is available free of charge via the Internet at http://pubs.acs.org.

IC020641Q

(56) Li, N.; Xiang, S. H. *J. Mater. Chem.* **2002**, *12*, 1397.
(57) Soghomonian, V.; Haushalter, R. C.; Zubieta, J. *Chem. Mater.* **1995**, *7*, 1648.